OXYGEN ISOTOPE VARIATION WITH CRYSTAL GROWTH OBSERVED IN ALLENDE COARSE-GRAINED TYPE B CAI TS34 -REVISITED-. N. Kawasaki[1], H. Yurimoto[1], S. B. Simon[2] and L. Grossman[2], [1]Natural History Sci. Hokkaido Univ., Sapporo 001-0021 Japan (yuri@ep.sci.hokudai.ac.jp), [2]Dept. of Geophysical Sci., Univ. of Chicago, Chicago, IL 60637 USA.

Introduction: The Allende type B1 CAI TS34 is one of the most well-studied CAIs in the solar system [1]. In typical CAI fashion, oxygen isotopes are distributed heterogeneously among the constituent minerals along a slope-1 line on an oxygen three-isotope diagram. Although TS34 has an igneous texture, oxygen isotope trends among the minerals do not follow the equilibrium crystallization sequence expected for CAI melt composition [2]. It is not easy to see how the oxygen isotope heterogeneity could have been caused by oxygen isotope exchange by solid-state diffusion after CAI solidification because of the oxygen self-diffusivities in the minerals [3, 4]. In fact, oxygen isotopes measured in Al-Ti-rich clinopyroxene in another coarse-grained type B CAI with intermediate ^{16}O-enrichment did not show any diffusion exchange profile for oxygen isotopes [5]. Evidence of oxygen isotope exchange during melting and recrystallization by temporal heating in the solar nebula is observed within melilite crystals in coarse-grained type A CAIs [6, 7]. Here, we revisit the TS34 CAI to measure the oxygen isotope distribution with careful petrographic control, and propose a new mechanism to form the oxygen isotopic distribution observed in the CAI.

Experimental methods: The Type B1 CAI, TS34, is included in a polished thin section of the Allende CV3 carbonaceous chondrite. The polished thin section was coated with a carbon thin film (~20 nm) for backscattered electron (BSE) imaging and elemental analysis using an energy dispersive X-ray spectrometer (EDS), and coated with a gold thin film (~70 nm) for oxygen isotope measurements using SIMS.

BSE images were obtained using a field emission type scanning electron microscope (FE-SEM; JEOL JSM-7000F) at Hokkaido University. Quantitative elemental analysis and X-ray elemental mapping were conducted using an energy-dispersive spectrometer (EDS, Oxford X-Max 150) installed on the FE-SEM.

Oxygen isotopic compositions of the minerals in TS34 were measured using the SIMS instrument (Cameca ims-1280HR) at Hokkaido University. A $^{133}Cs^+$ primary beam (20 keV, 60 pA) with a diameter of 2–3 μm was used. Negative secondary ions were measured simultaneously in the multicollection mode. A normal incident electron flood gun was used for the electrostatic charge compensation. The mass resolution $M/\Delta M$ for $^{17}O^-$ was set at ~6000, while that for $^{16}O^-$ and $^{18}O^-$ was ~2000. The intensity ratios measured were corrected to δ-SMOW values using terrestrial standards.

Results and Discussion: The TS34 CAI mainly consists of melilite, Al-Ti-rich clinopyroxene and spinel [1, 8-11] in an igneous texture. Oxygen isotopic compositions of the minerals plot along a slope-1 line (Fig. 1). Spinel is ^{16}O-rich, whereas melilite ^{16}O-poor, which are consistent with previous results [1, 9]. On the other hand, Al-Ti-rich clinopyroxene crystals have various degrees of ^{16}O-enrichments between O isotopic compositions of spinel and melilite. In order to clarify systematics of the oxygen isotopic variation, we mapped the spatial heterogeneity of the oxygen isotopes within a pyroxene crystal.

Blocky Al-Ti-rich clinopyroxene crystals are abundant in TS34 CAI. Chemical zoning of Ti reveals the direction of crystal growth. The pyroxene grew from Ti-rich to Ti-poor compositions with gradual chemical zoning as shown in the contour lines of Fig. 2. Oxygen isotopic compositions were measured along lines A-B and A-C traversing crystal growth contours. Point A corresponds to the start of crystal growth and points B and C correspond to the ends of crystal growth for the pyroxene.

The pyroxene crystal covers the entire variation range of oxygen isotopic compositions observed in the TS34 CAI. Crystal growth began with an ^{16}O-poor composition that is isotopically in equilibrium with

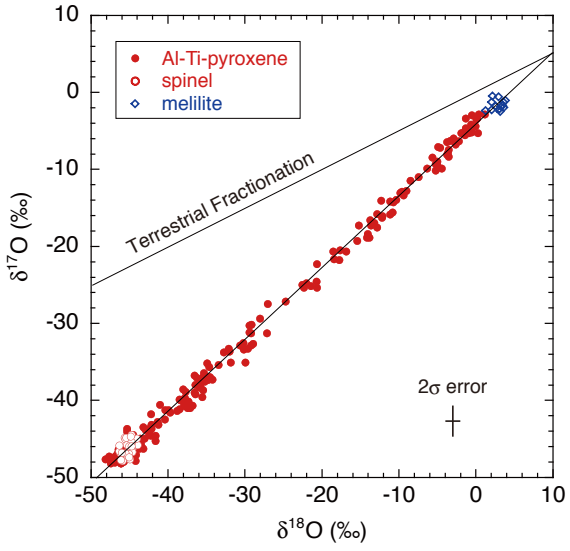

Fig. 1. Oxygen isotope compositions of minerals in TS34.

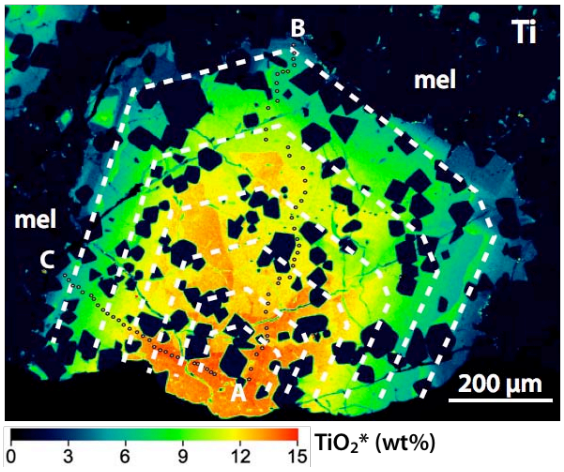

Fig. 2. Ti elemental map of Al-Ti-rich clinopyroxene in TS34. The pyroxene contains spinel (black) inclusions and is surrounded by melilite (black). Dashed lines show growth contours. Small dots between A-B and A-C show measurement points for O isotope analysis.

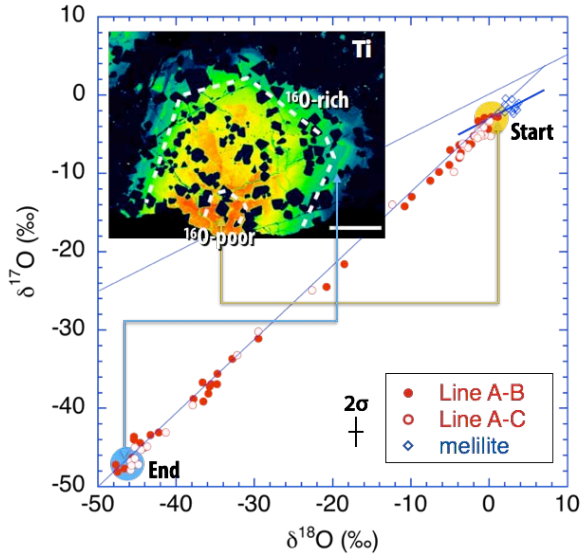

Fig. 3. Oxygen isotope variation within the clinopyroxene crystal shown in Fig. 2. Lines A-B and A-C are shown in Fig. 2. The crystal started ^{16}O-poor (inside inner growth contour) and ended ^{16}O-rich (outside outer contour).

melilite (Fig. 3). As the crystal grew, the oxygen isotopic composition gradually became ^{16}O-rich along the slope-1 line and approached the solar O isotopic signature [12-14]. The bulk O isotopic composition of pyroxene is relatively ^{16}O-rich, consistent with results from mineral separates [1], because the volume proportion of ^{16}O-poor compositions is relatively small.

The oxygen isotopic distribution in pyroxene correlates with the O isotopic evolution of the liquid in the CAI. The oxygen isotopic composition of the liquid was ^{16}O-poor when the liquid equilibrated with melilite and the earliest pyroxene. The^{16}O-rich spinel are relict crystals [2] that preserve a record of isotopic disequilibrium. As the temperature fell, the liquid crystallized pyroxene with increasingly ^{16}O-rich composition. The ^{16}O-rich signature must have been introduced from outside the CAI because there are no available reservoirs within the CAI. The surrounding gas is the most plausible candidate for the ^{16}O-rich source because O is the most abundant element in the gas after H and He. Oxygen isotopic variation of the gas surrounding CAIs is supported by measurements of directly condensed minerals of CAIs [15-19]. The oxygen isotopic variations observed in the TS34 CAI suggest that the gas changed cyclically from ^{16}O-rich (spinel), ^{16}O-poor (melilite, early pyroxene) and then ^{16}O-rich(late pyroxene) in the early solar system. Oxygen isotopic contrast between the Sun and the solar protoplanetary disk, i.e., having solar and planetary signatures, respectively, has been derived by a model [20]. A boundary between the contrasting reservoirs may have existed at the inner edge of the protoplanetary disk [21]. Preservation of oxygen isotopic variations requires melting and recrystallization that may have been caused by giant flares from the protosun [22].

References: [1] Clayton, R.N. et al. (1977) *Earth Planet. Sci. Lett. 34*, 209-224. [2] Stolper, E. (1982) *Geochim. Cosmochim. Acta 46*, 2159-2180. [3] Yurimoto, H. et al. (1989) *Geochim. Cosmochim. Acta 53*, 2387-2394. [4] Ryerson, F.G. and McKeegan, K.D. (1994) *Geochim. Cosmochim. Acta 58*, 3713-3734. [5] Yurimoto, H. et al. (1994) *Earth Planet. Sci. Lett. 128*, 47-53. [6] Yurimoto, H. et al. (1998) *Science 282*, 1874-1877. [7] Aléon, J. et al. (2007) *Earth Planet. Sci. Lett. 263*, 114-127. [8] Simon, S.B. et al. (1991) *Geochim. Cosmochim. Acta 55*, 2635-2655. [9] Connolly, H.C. et al. (2003) *Meteorit. Planet. Sci. 38*, 197-224. [10] Simon, S.B. and Grossman, L. (2006) *Geochim. Cosmochim. Acta 70*, 780-798. [11] Paque, J.M. et al. (2013) *Meteorit. Planet. Sci. 48*, 2015-2043. [12] Kobayashi, S. et al. (2003) *Geochem. J. 37*, 663-669. [13] Fujimoto, K. et al. (2009) *Geochem. J.* 43, e11-e15. [14] McKeegan, K.D. et al. (2011) *Science 332*, 1528-1532. [15] Yoshitake, M. et al. (2005) *Geochim. Cosmochim. Acta 69*, 2663-2674. [16] Simon, J. I. et al. (2011) *Science 331*, 1175-1178. [17] Katayama, J. et al. (2012) *Meteorit. Planet. Sci. 47*, 2094–2106. [18] Kawasaki, N. (2012) *Meteorit. Planet. Sci. 47*, 2084–2093. [19] Park, C. (2012) *Meteorit. Planet. Sci. 47*, 2070–2083. [20] Yurimoto, H. and Kuramoto, K. (2004) *Science 305*, 1763-1766. [21] Yurimoto, H. et al. (2008) *Rev. Mineral. Geochem. 68*, 141-186. [22] Nakamoto, T. et al. (2005) in: Krot, A.N., Scott, E.R.D., Reipurth, B. (Eds.), *Chondrules and the Protoplanetary Disk*, pp. 883-892.